Supporting Information

Vaeth et al. 10.1073/pnas.1409290112

SI Materials and Methods

Mice. *Nfat1*$^{-/-}$ mice (1) were kindly provided by L. Glimcher (Harvard School of Public Health, Boston). *Nfat2*$^{fl/fl}$ animals (2, 3) were engineered and generously allocated by A. Rao (La Jolla Institute for Allergy and Immunology, La Jolla, CA). *Tcrb*$^{-/-}$ *Tcrd*$^{-/-}$ mice (4) were a kind gift of C. Krempl (University of Würzburg, Würzburg, Germany) and DEREG (5) were provided by T. Sparwasser (Twincore, Hanover, Germany). B6-Tg (*Cd4cre*) 1Cwi/Cwilbcm were obtained from the European Mouse Mutant Archive (6). B6.L2G85.CD90.1 transgenic mice ubiquitously expressing firefly luciferase and CD90.1 as a congenic marker were described in detail before (7). All mice were on C57BL/6 background (H-2^b) and female animals were used for experiments between 8 and 12 wk of age. All mice were bred within the specified pathogen-free animal facility of the Center for Experimental Molecular Medicine (ZEMM) at the University of Würzburg. Female CD90.2$^+$ C57BL/6 (H-2^b), BALB/c (H-2^d), and CB6F1 (C57BL6 × BALB/c F1 hybrid; H-2^{b+d}) WT recipient mice were purchased from Charles River. All animal experiments were approved by the respective authorities (Regierung von Unterfranken) and compiled with German animal protection law.

Tumor Cells. Myc-driven B-cell lymphoma IM380 and A20 yfp/luc leukemia B cells (both H-2^d background) were described before (8, 9). Both cell lines express firefly luciferase (luc$^+$) and were maintained in exponential growth phase in complete RPMI medium containing 10% (vol/vol) FCS (Life Technologies). Ovalbumin-expressing C57BL/6 B16F10 (B16F10^{OVA}) murine melanoma cells (H-2^b) were maintained in complete RPMI medium containing 10% FCS (Life Technologies).

BM and T-Cell Isolation. BM cells were isolated by flushing femur and tibia bones with PBS containing 0.1% BSA and passed through a 70-μm cell strainer. In GvL experiments, T cells were depleted from BM suspensions using the CD4$^+$ and CD8$^+$ MicroBead kit (Miltenyi Biotec) according to manufacturer instructions. Spleens were directly passed through a 70-μm cell strainer with erythrocyte lysis buffer (168 mM NH_4Cl, 10 mM $KHCO_3$, 0.1 mM EDTA) and washed twice with PBS containing 0.1% BSA. T cells were enriched from WT, *Nfat1*$^{-/-}$, *Nfat2*$^{fl/fl}$ *Cd4cre*, and *Nfat1*$^{-/-}$*Nfat2*$^{fl/fl}$ *Cd4cre* splenocytes using the Dynal Mouse T-cell Negative Isolation kit (Life Technologies) according to the manufacturer's instructions. CD4$^+$CD25^{hi} nTregs were enriched by staining negatively isolated T cells with anti-CD25-PE (PC61, BD Pharmingen) and separation of CD4$^+$CD25^{hi} nTregs and CD4$^+$CD25$^-$ Tcon cells was performed using anti-PE MicroBeads (Miltenyi Biotech) following manufacturer instructions. Purity of the CD4$^+$CD25^{hi} or CD4$^+$CD25$^-$ population was typically >90% or 95%, respectively.

Allogenic Hematopoietic Stem Cell Transplantation. BALB/c host mice (H-2^d CD90.2$^+$) were conditioned by myeloablative total body irradiation (TBI) at a dose of 8.0 Gy using a Faxitron CP-160 X-ray system and injected retroorbitally with sex- and age-matched 5 × 10^6 C57BL/6 WT BM cells (H-2^b CD90.2$^+$) with or without 1.2 × 10^6 C57BL/6 total T cells or CD25-depleted Tcon (H-2^b CD90.1$^+$ luc$^+$) within 2 h after irradiation (Fig. S1*A*). For nTreg-mediated suppression of GvHD, BALB/c host mice (H-2^d CD90.2$^+$) were conditioned with a TBI dose of 8.0 Gy and injected retroorbitally with sex- and age-matched 5 × 10^6 C57BL/6 WT BM cells (H-2^b CD90.2$^+$) together with 6 × 10^5 C57BL/6 CD4$^+$CD25^{hi} nTregs (H-2^b CD90.2$^+$ luc$^-$). Twenty-four hours later, 1.2 × 10^6 C57BL/6 CD4$^+$CD25$^-$ Tcon (H-2^b CD90.1$^+$ luc$^+$) were injected i.v. (Fig. S6*A*). Mice were treated with antibiotic drinking water (Baytril, Bayer) for 7 d after allogenic hematopoietic stem cell transplantation (allo-HCT) to prevent unspecific infections. Transplanted mice were assessed daily for weight loss and clinical scoring for GvHD symptoms (adapted from Cooke et al., ref. 10).

Depletion of Tregs After Allo-HCT. BALB/c host mice (H-2^d) were conditioned by myeloablative TBI at a dose of 8.0 Gy and injected retroorbitally with 5 × 10^6 C57BL/6 *Tcrb*$^{-/-}$*Tcrd*$^{-/-}$ BM cells (H-2^b CD90.2$^+$) together with 1.2 × 10^6 C57BL/6 WT × DEREG (*Foxp3*^{DTR} tg) or 1.2 × 10^6 C57BL/6 *Nfat1*$^{-/-}$ × DEREG T cells (Fig. 3*H*). To deplete Tregs, 1 μg diphtheria toxin (DTx, Merck) per mouse was injected i.p. at days 1, 2, and 3 after allo-HCT; control mice received 100 μL PBS. Mice were treated with antibiotic drinking water (Baytril, Bayer) for 7 d after allo-HCT to prevent unspecific infections.

Tumor Models. For the Myc-driven B-cell lymphoma IM380 model, 2.5 × 10^4 IM380 tumor cells (luc$^+$ H-2^d) were injected into the lateral tail vein of syngenic BALB/c host mice. Six days later, mice were conditioned with a TBI dose of 8.0 Gy and injected retroorbitally with sex- and age-matched 5 × 10^6 C57BL/6 WT BM cells (H-2^b CD90.2$^+$) with or without 1.2 × 10^6 C57BL/6 T cells (H-2^b CD90.1$^+$ luc$^-$) within 2 h after irradiation (Fig. S7*A*). For the A20 yfp/luc leukemia B cells model, BALB/c host mice (H-2^d CD90.2$^+$) were conditioned with a TBI dose of 8.0 Gy, and 2 × 10^4 syngenic A20 tumor cells (luc$^+$ H-2^d) were injected into the lateral tail vein. Twenty-four hours later, mice were injected retroorbitally with sex-matched 5 × 10^6 C57BL/6 WT T-cell–depleted BM cells (H-2^b CD90.2$^+$) with or without 1.2 × 10^6 C57BL/6 T cells (H-2^b CD90.1$^+$ luc$^-$) (Fig. S8*A*). Mice were treated with antibiotic drinking water (Baytril, Bayer) for 7 d after allo-HCT to prevent unspecific infections. Transplanted mice were assessed daily for weight loss and clinical scoring for tumor and GvHD symptoms (adapted from ref. 10).

CD8 T-Cell Memory Response After Semiallogenic HCT. C57BL/6 WT and NFAT-deficient mice were immunized with 100 μg OVA SIINFEKL peptide (Biozol) plus 50 μg CpG (ODN 1826 VacciGrade, Invivogen) emulsified in incomplete Freund's adjuvant (IFA, Invivogen) s.c. into the tail base. Nine days later, 1.2 × 10^6 T cells from SIINFEKL-immunized C57BL/6 mice (H-2^b) together with 5 × 10^5 BM cells from *Tcrb*$^{-/-}$*Tcrd*$^{-/-}$ C57BL/6 mice were transplanted retroorbitally into sex-matched semiallogenic CB6F1 (H-2^{b+d}) mice. CB6F1 host mice are the F1 hybrid of C57BL/6 × BALB/c crossings (providing a semiallogenic immunological environment, but being able to present peptides on C57BL/6-restricted H-2^b molecules). CB6F1 hosts were conditioned before with a single dose of 9.0 Gy TBI. On days 1 and 2 after semiallo-HCT, host mice were boosted i.v. with 100 μg SIINFEKL peptide (Fig. S10*C*). Memory response of OVA-specific CD8$^+$ T cells was tested 4 d later by coculturing 4 × 10^4 splenic T cells with 5 × 10^3 OVA-expressing B16F10 melanoma cells (B16F10^{OVA}) for 4 h in 96 U-bottom well plates. Dead B16F10 cells were analyzed by propidium iodide staining using flow cytometry.

In Vivo and ex Vivo Bioluminescence Imaging. Mice were anesthetized by i.p. injection of 80 mg/kg body weight ketamine hydrochloride (Pfizer) and 16 mg/kg xylazine (CP Pharma). Together with anesthetics, mice were injected with 150 mg/kg D-luciferin (Biosynth). After 10 min, BLI signals of the anesthetized mice were recorded using an IVIS Spectrum Imaging system (Caliper Life Sciences).

For ex vivo imaging of internal organs 6 d after allo-HCT, mice were injected with D-luciferin and killed 10 min later. Internal organs were removed and subjected to BLI. All pictures were taken with a maximum of 5-min exposure time and analyzed with the Living Image 4.0 software (Caliper Life Sciences).

Flow Cytometry. Cells were washed once in FACS buffer (PBS containing 0.1% BSA) before blocking with anti-FcγRII/FcγRIII (2.4G2, BD Pharmingen). Staining of surface molecules was performed on ice using FITC-conjugated CD4 (RM4-5), CD8α (53-6.7), and CD90.1 (OX-7); PE-conjugated α4β7 (LPAM-1, DATK32), CD4 (RM4-5), CD8α (53-6.7), and CD25 (PC61), CD107a (eBio1D4B), granzyme B (NGZB), FasL (MFL3); APC-conjugated CD8α (53-6.7), CD40L (MR1), CD90.1 (OX-7), and perforin (eBioOMAK-D); and eFluor450-conjugated CD4 (RM4-5) and CD103 (2E7) mAbs (all eBioscience or BioLegend) in FACS buffer for 20 min in the dark. Similarly, staining of splenic T cells with the APC-conjugated iTAg MHC class I (H-2k^b) OVA (SIINFEKL) tetramer (MoBiTech) was performed for 45 min and fixed afterward with IC Fixation Buffer kit (eBioscience). Intracellular Foxp3 (FJK-16s, PE or APC conjugated; eBioscience) staining was performed using the Foxp3 Staining kit (eBioscience) according to the manufacturer's instructions. Intracellular cytokine staining of splenocytes with APC-conjugated IL-2 (JES6-5H4), IFNγ (XMG1.2), IL-10 (JES5-16E3), and PE-conjugated IL-4 (11B11), IL-17 (eBio17B7), TNFα (MP6-XT22; all eBioscience) was performed after 6-h restimulation in vitro with 12-*O*-tetradecanoylphorbol-13-acetate (TPA; 10 ng/mL, Sigma) plus ionomycin (5 nM, Merck Biosciences) in the presence of GolgiStop and GolgiPlug (both BD Pharmingen) using the IC Fixation Buffer kit (eBioscience). Viable cells were detected with the LIVE/DEAD Fixable Violet Dead Cell Stain kit (Life Technologies). Data were acquired on a FACS Canto II (BD Biosciences) flow cytometer and analyzed with FlowJo software (Tree Star).

CFSE in Vivo Proliferation Assay. BALB/c host mice (H-2^d CD90.2$^+$) were conditioned with a TBI dose of 8.0 Gy and injected retroorbitally with sex- and age-matched 5×10^6 C57BL/6 WT BM cells (H-2^b CD90.2$^+$) together with 1.2×10^6 CFSE-labeled (Molecular Probes) C57BL/6 T cells (H-2^b CD90.1$^+$) within 2 h after irradiation. Three days after allo-HCT, spleen and LNs (mesenteric, inguinal, and cervical) were isolated and CFSE dilution of allogenic CD90.1$^+$CD4$^+$ and CD90.1$^+$CD8$^+$ donor T cells was measured using a FACS Canto II (BD Biosciences) flow cytometer.

Cytometric Bead Array. Serum cytokine concentrations were determined using the Mouse T_H1/T_H2 Cytometric Bead Array kit (BD Pharmingen) according to the manufacturer's protocol 6 d after allo-HCT. Data were acquired on a FACS Canto II (BD Biosciences) flow cytometer and analyzed with FCAP Array v2.0 software.

Quantitative qRT-PCR. RNA was extracted from total splenocytes or FACS-sorted CD44$^-$CD62L^{hi} naïve or CD44^{hi}CD62L$^-$ effector CD4$^+$ and CD8$^+$ T cells using the RNeasy Micro kit (Qiagen) followed by cDNA synthesis with the iScript II kit (BioRad). Quantitative RT-PCR was performed with an ABI Prism 770 light cycler with the following primer pairs:

Nfat1, TCATAGGAGCCCGACTGATTG plus CCATTCCCATCTGCAGCAT;

Nfat2 P1 product, CGGGAGCGGAGAAACTTTGC plus CAGGGTCGAGGTGACACTAG; *Nfat2 P2 product*, AGGACCCGGAGTTCGACTTC plus CAGGGTCGAGGTGACACTAG; *Nfat4*, GCCTCCATTGACAGAGCAACT plus CACATCCCACAGCCCAGTG;

Foxp3, GGCCCTTCTCCAGGACAGA plus GCTGATCATGGCTGGGTTGT;

Cd4, CAAGCGCCTAAGAGAGATGG plus CACCTGTGCAAGAAGCAGAG;

Hprt, AGCCTAAGATGAGCGCAAGT plus TTACTAGGCAGATGGCCACA.

Histopathology and Immunohistochemistry. Formalin-fixed, paraffin-embedded tissue specimens were prepared and hematoxylin and eosin (H&E) staining was performed as previously described (3). Colon, small bowel, liver, lungs, and skin from mice 12 d after allo-HCT were reviewed by an unbiased and experienced pathologist (A.M.). The following scoring (0–4 depending on severity) was used: small bowel/large bowel: crypt apoptosis, crypt destruction, and inflammation; liver: bile duct injury, vascular injury, hepatocellular damage, and portal inflammation; lungs: periluminal infiltrate and pneumonitis; and skin: apoptosis, ballooning of the basal layer, and inflammation (score 0–3). Representative images were obtained with a DP26 camera (Olympus) and cellSens Entry 1.5 software, version XV 3.5. For multicolor immunofluorescence staining, heat-induced antigen retrieval was performed under pressure in citrate buffer (pH 6.0; Sigma). The following primary antibodies were used: rabbit anti-CD3ε (DAKO) and rat anti-Foxp3 (FJK-16s, eBiosciences). Secondary staining was performed using polyclonal anti-rabbit Alexa Fluor 488 and anti-rat Alexa Fluor 555 goat Abs (both Molecular Probes). Slides were mounted with Fluoromount-G (Southern Biotechnology) containing DAPI. Images were taken with a confocal microscope (Leica TCS SP2 equipment, objective lense; HeX PL APO, 40×/1.25–0.75) and analyzed with LCS software (Leica). For statistics, more than 100 cells from five independent samples were evaluated.

Statistical Analyses. All data are shown as mean ± SE of mean and represent combined data from at least three independent experiments unless otherwise noted. Figures were prepared using GraphPad Prism 5, Adobe Photoshop, and Adobe Illustrator software. Different groups were compared by two-tailed Student's *t* test or two-way ANOVA as indicated in the figure legends using GraphPad Prism 5 software.

1. Hodge MR, et al. (1996) Hyperproliferation and dysregulation of IL-4 expression in NF-ATp-deficient mice. *Immunity* 4(4):397–405.
2. Oh-Hora M, et al. (2013) Agonist-selected T cell development requires strong T cell receptor signaling and store-operated calcium entry. *Immunity* 38(5): 881–895.
3. Vaeth M, et al. (2012) Dependence on nuclear factor of activated T-cells (NFAT) levels discriminates conventional T cells from Foxp3+ regulatory T cells. *Proc Natl Acad Sci USA* 109(40):16258–16263.
4. Mombaerts P, et al. (1992) Mutations in T-cell antigen receptor genes alpha and beta block thymocyte development at different stages. *Nature* 360(6401):225–231.
5. Lahl K, et al. (2007) Selective depletion of Foxp3+ regulatory T cells induces a scurfy-like disease. *J Exp Med* 204(1):57–63.
6. Lee PP, et al. (2001) A critical role for Dnmt1 and DNA methylation in T cell development, function, and survival. *Immunity* 15(5):763–774.
7. Beilhack A, et al. (2005) In vivo analyses of early events in acute graft-versus-host disease reveal sequential infiltration of T-cell subsets. *Blood* 106(3):1113–1122.
8. Chopra M, et al. (2013) Non-invasive bioluminescence imaging to monitor the immunological control of a plasmablastic lymphoma-like B cell neoplasia after hematopoietic cell transplantation. *PLoS ONE* 8(12):e81320.
9. Edinger M, et al. (2003) Revealing lymphoma growth and the efficacy of immune cell therapies using in vivo bioluminescence imaging. *Blood* 101(2):640–648.
10. Cooke KR, et al. (1996) An experimental model of idiopathic pneumonia syndrome after bone marrow transplantation: I. The roles of minor H antigens and endotoxin. *Blood* 88(8):3230–3239.

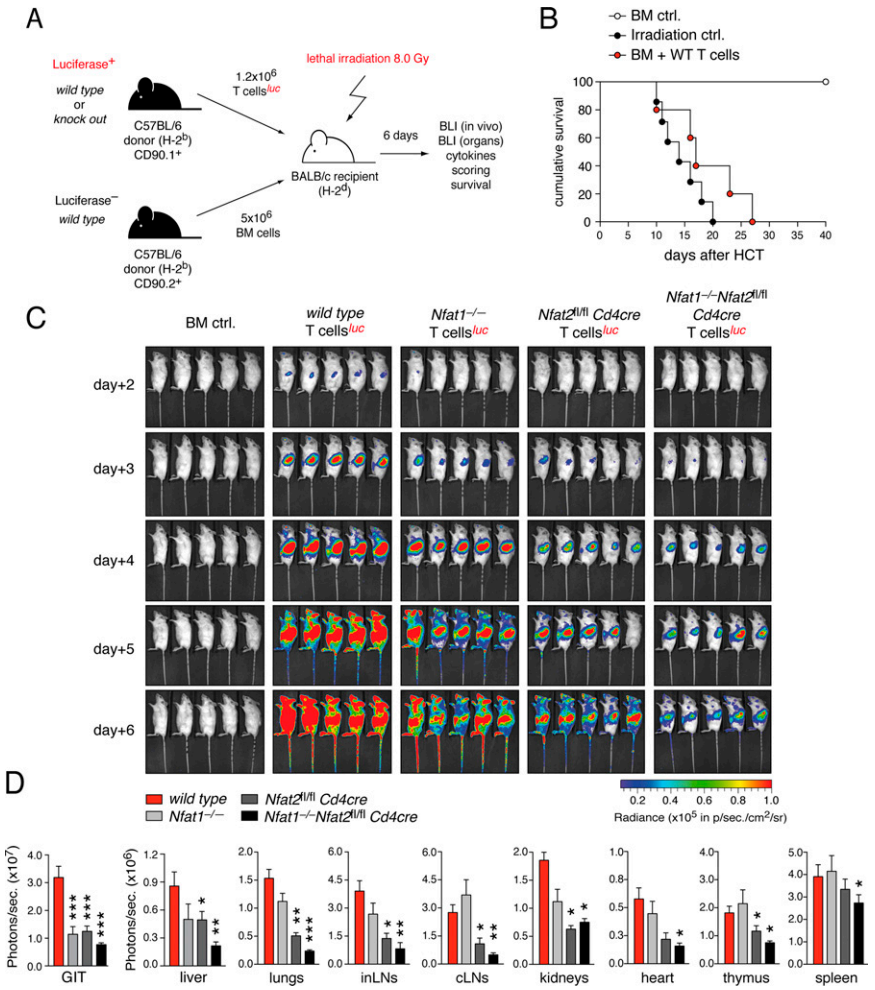

Fig. S1. NFAT-deficient T cells show impaired expansion and target organ infiltration after allo-HCT. (*A*) Preclinical model of acute GvHD after MHC-mismatched allo-HCT. BALB/c (H-2^d) mice were lethally irradiated with a single dose of 8.0 Gy and transplanted with 5×10^6 CD90.2^+ BM cells and 1.2×10^6 CD90.1^+luciferase$^+$ T cells from C57BL/6 donors (H-2^b). (*B*) Cumulative survival of irradiated BALB/c mice without any transfer of cells (Irradiation ctrl), with transfer of 5×10^6 BM cells from C57BL/6 donor mice (BM ctrl), or transfer of 5×10^6 BM cells plus 1.2×10^6 T cells (BM + Tcon) from WT C57BL/6 donor mice. Median survival: BM ctrl: >40 d; irradiation ctrl: 14 d; WT T cells median survival: 17 d. (*C*) Representative in vivo bioluminescence imaging (BLI) of mice transplanted with 1.2×10^6 luciferase WT, *Nfat1*$^{-/-}$, *Nfat2*$^{fl/fl}$ *Cd4cre*, and *Nfat1*$^{-/-}$*Nfat2*$^{fl/fl}$ *Cd4cre* T cells plus 5×10^6 BM cells. (*D*) Quantification of ex vivo BLI data from internal organs 6 d after the transfer of 1.2×10^6 luciferase$^+$ WT, *Nfat1*$^{-/-}$, *Nfat2*$^{fl/fl}$ *Cd4cre*, and *Nfat1*$^{-/-}$*Nfat2*$^{fl/fl}$ *Cd4cre* T cells. Data are compiled from at least two independent experiments with five mice per group per experiment. Statistical significance was calculated using Student's *t* test (*D*); $*P < 0.05$, $**P < 0.01$, $***P < 0.001$.

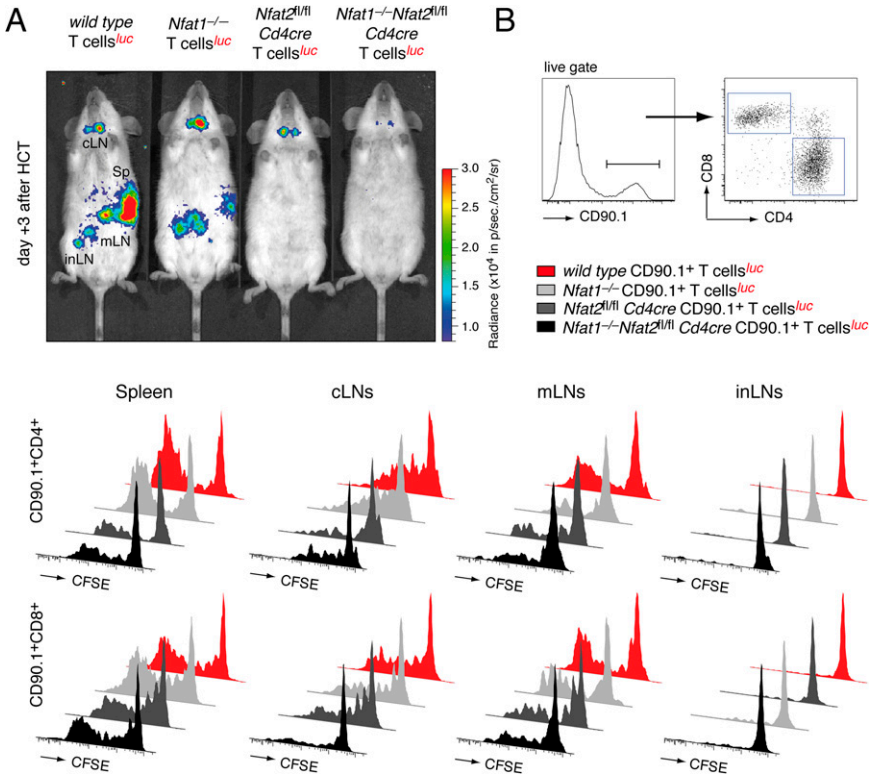

Fig. S2. NFAT-deficient CD4$^+$ and CD8$^+$ T cells show reduced proliferation after allo-HCT. (*A*) Representative in vivo BLI data of mice transplanted with 1.2 × 10^6 CD90.1$^+$ luciferase$^+$ WT, *Nfat1*$^{-/-}$, *Nfat2*$^{fl/fl}$ *Cd4cre*, and *Nfat1*$^{-/-}$*Nfat2*$^{fl/fl}$ *Cd4cre* T cells along with 5 × 10^6 CD90.2$^+$ BM cells 3 d after allo-HCT. (*B*) Identification of CD90.1$^+$ donor CD4$^+$ and CD8$^+$ T cells in various lymphoid organs of recipient mice using flow cytometry (*Upper*). Proliferation of CSFE-labeled CD90.1$^+$ WT, *Nfat1*$^{-/-}$, *Nfat2*$^{fl/fl}$ *Cd4cre*, and *Nfat1*$^{-/-}$*Nfat2*$^{fl/fl}$ *Cd4cre* T cells in cervical LNs (cLNs), inguinal LNs (inLNs), mesenteric LNs (mLNs), and spleen 3 d after allo-HCT analyzed by flow cytometry (*Lower*).

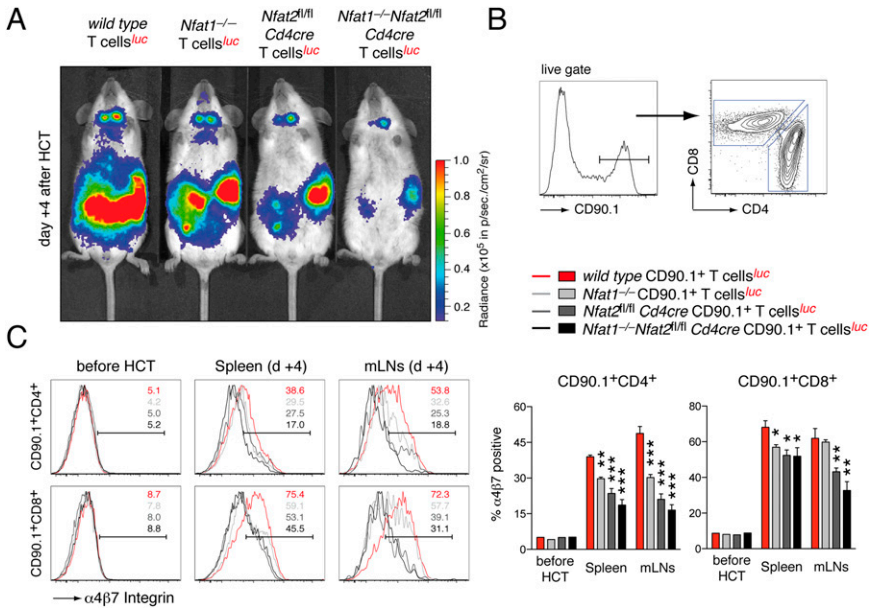

Fig. S3. NFAT-deficient CD4$^+$ and CD8$^+$ T cells show impaired up-regulation of homing receptor α4β7 integrin after allo-HCT. (*A*) Representative in vivo BLI data of mice transplanted with 1.2 × 10^6 CD90.1$^+$ luciferase$^+$ WT, *Nfat1*$^{-/-}$, *Nfat2*$^{fl/fl}$ *Cd4cre*, and *Nfat1*$^{-/-}$*Nfat2*$^{fl/fl}$ *Cd4cre* T cells along with 5 × 10^6 CD90.2$^+$ BM cells 4 d after allo-HCT. (*B*) Identification of CD90.1$^+$ donor CD4$^+$ and CD8$^+$ T cells in spleen and mLNs of recipient mice using flow cytometry. (*C*) Analysis of α4β7 integrin expression on CD90.1$^+$ WT, *Nfat1*$^{-/-}$, *Nfat2*$^{fl/fl}$ *Cd4cre*, and *Nfat1*$^{-/-}$*Nfat2*$^{fl/fl}$ *Cd4cre* donor CD4 and CD8 T cells before and 4 d after allo-HCT in spleen and mesenteric LNs measured by flow cytometry; data from three individual recipient mice were summarized (*Lower Right*). Statistical significance was calculated using two-way ANOVA; *P < 0.05, **P < 0.01, ***P < 0.001.

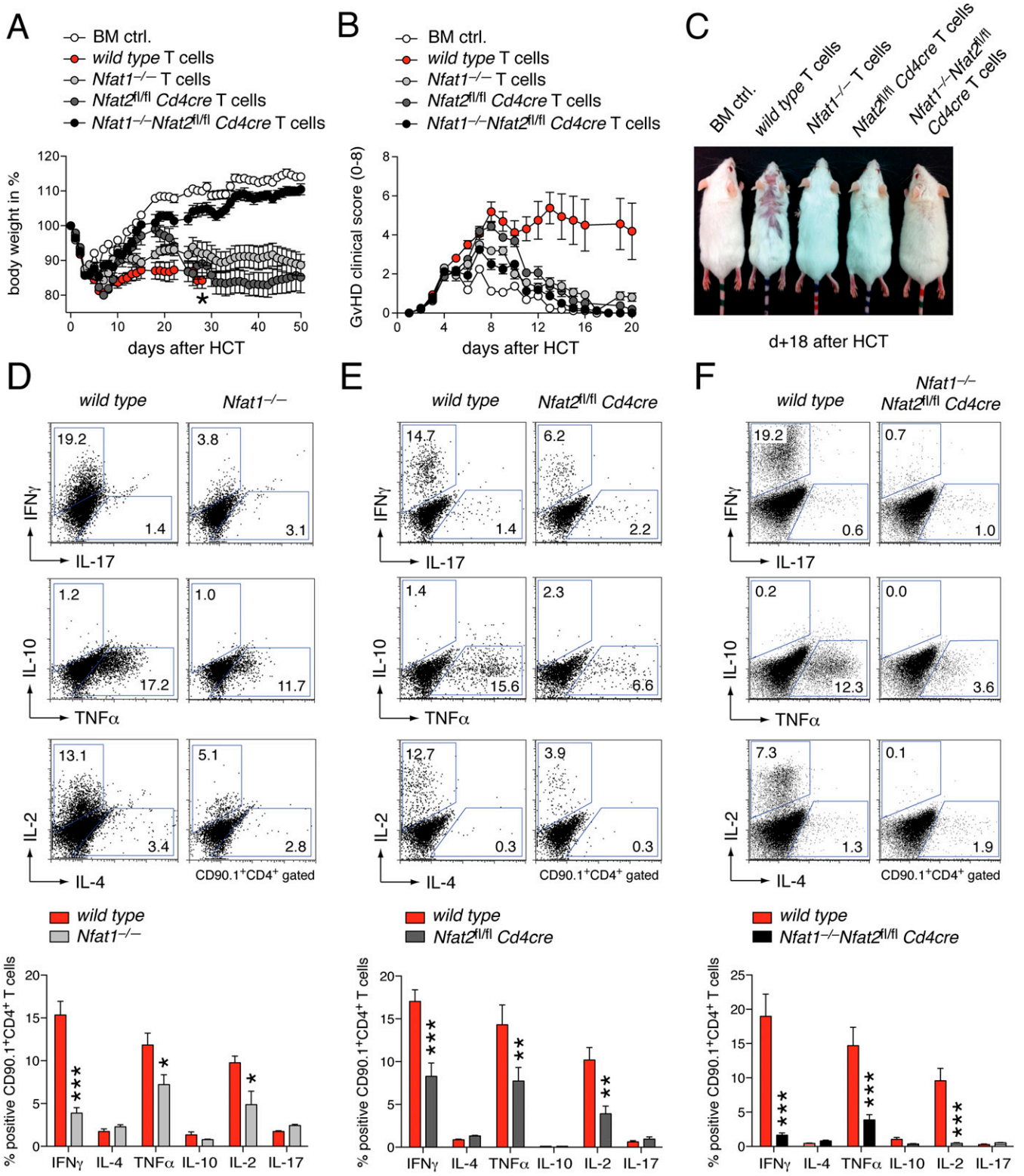

Fig. S4. NFAT-deficient T cells do not cause fatal GvHD pathology and NFAT-deficient donor CD4$^+$ T cells express reduced proinflammatory cytokines. (*A*) Body weight changes of host BALB/c mice transplanted with 1.2×10^6 allogenic WT ($n = 8$), *Nfat1*$^{-/-}$, *Nfat2*$^{fl/fl}$ *Cd4cre* ($n = 8$), or *Nfat1*$^{-/-}$*Nfat2*$^{fl/fl}$ *Cd4cre* ($n = 8$) T cells plus 5×10^6 BM cells over a course of 50 d. Control mice (BM ctrl; $n = 8$) received only 5×10^6 BM cells. Asterisk: all mice of the WT group died due to acute GvHD pathology. (*B*) Clinical GvHD scoring (score 0–8) of mice transplanted with 1.2×10^6 allogenic WT ($n = 8$), *Nfat1*$^{-/-}$ ($n = 10$), *Nfat2*$^{fl/fl}$ *Cd4cre* ($n = 6$), and *Nfat1*$^{-/-}$*Nfat2*$^{fl/fl}$ *Cd4cre* T cells ($n = 7$) plus 5×10^6 BM cells; control mice (BM ctrl; $n = 8$) received only 5×10^6 BM cells. (*C*) Representative picture showing GvHD pathology in host BALB/c mice transplanted with 1.2×10^6 WT, *Nfat1*$^{-/-}$, *Nfat2*$^{fl/fl}$ *Cd4cre*, and *Nfat1*$^{-/-}$*Nfat2*$^{fl/fl}$ *Cd4cre* T cells 18 d after allo-HCT. (*D*) Representative intracellular flow cytometry detecting cytokine expression of splenic CD90.1$^+$CD4$^+$ WT and *Nfat1*$^{-/-}$ donor T cells 6 d after allo-HCT (*Upper*). Total spleen cells were restimulated for 6 h with TPA/ionomycin. Quantification of data from five mice per group (*Lower*). (*E*) Representative intracellular flow

Legend continued on following page

cytometry detecting cytokine expression by splenic CD90.1$^+$CD4$^+$ WT and *Nfat2*$^{fl/fl}$ *Cd4cre* donor T cells 6 d after allo-HCT (*Upper*). Summary of data derived from five individual mice per group (*Lower*). (*F*) Representative intracellular flow cytometry detecting cytokine expression of splenic CD90.1$^+$CD4$^+$ WT and *Nfat1*$^{-/-}$*Nfat2*$^{fl/fl}$ *Cd4cre* donor T cells 6 d after allo-HCT (*Upper*). Summary of data derived from five individual mice per group (*Lower*). Statistical significance was calculated using Student's *t* test (*A*–*C*); *$P < 0.05$, **$P < 0.01$, ***$P < 0.001$.

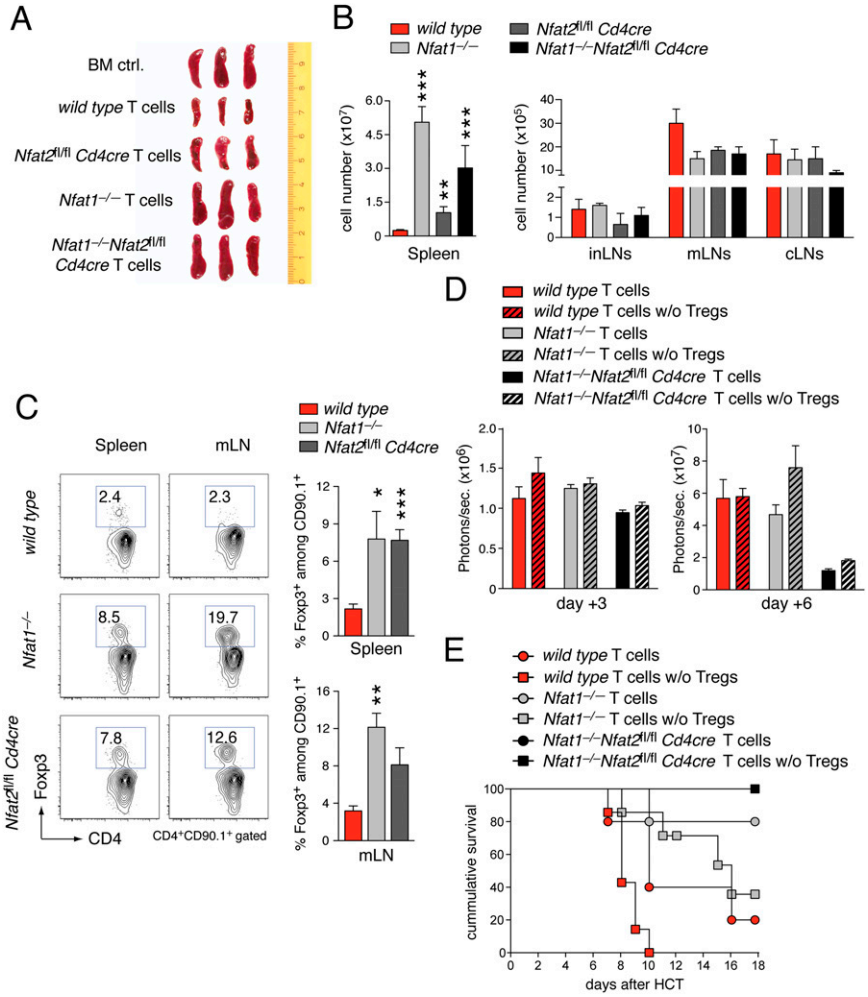

Fig. S5. Transplantation of NFAT-deficient T cells reconstitutes normal cellularity of secondary lymphoid organs. (*A*) Representative picture showing size and pathology of spleens from host mice 12 d after allo-HCT. Mice were transplanted with 1.2×10^6 allogenic WT, *Nfat1*$^{-/-}$, *Nfat2*$^{fl/fl}$ *Cd4cre*, and *Nfat1*$^{-/-}$*Nfat2*$^{fl/fl}$ *Cd4cre* T cells together with 5×10^6 BM cells and spleen pathology was assessed 12 d later. (*B*) Cellularity of spleens as shown in *A* and different LNs (inguinal LNs, mesenteric LNs, and cervical LNs); data are compiled from two independent experiments with five mice per group for the spleens and three mice per group from one experiment for the LNs. (*C*) Analysis of CD90.1$^+$CD4$^+$Foxp3$^+$ donor-derived Treg frequency in spleen and mLN 12 d after the transfer of 1.2×10^6 WT, *Nfat1*$^{-/-}$, or *Nfat2*$^{fl/fl}$ *Cd4cre* T cells by flow cytometry (*Left*); data are quantified from two independent experiments with five mice per group (*Right*). (*D*) BALB/c mice were transplanted with 1.2×10^6 luciferase$^+$ T cells with or depleted for CD4$^+$CD25^{hi} Tregs (w/o Tregs) from WT, *Nfat1*$^{-/-}$, or *Nfat1*$^{-/-}$ *Nfat2*$^{fl/fl}$ *Cd4cre* C57BL/6 donors together with 5×10^5 BM cells. Ventral in vivo BLI data on days 3 (*Left*) and 5 after allo-HCT (*Right*) were summarized from five to seven mice per group as described in Fig. 1 *A* and *B*. (*E*) Cumulative survival of BALB/c mice transplanted with 1.2×10^6 luciferase$^+$ T cells with or w/o CD4$^+$CD25^{hi} nTregs from WT ($n = 5$–7), *Nfat1*$^{-/-}$ ($n = 5$–7), or *Nfat1*$^{-/-}$ *Nfat2*$^{fl/fl}$ *Cd4cre* ($n = 5$) donors. Median survival: WT T cells: 10 d; WT T cells w/o Tregs: 8 d; *Nfat1*$^{-/-}$ T cells w/o Tregs: 16 d; *Nfat1*$^{-/-}$ T cells, *Nfat1*$^{-/-}$*Nfat2*$^{fl/fl}$ *Cd4cre* T cells, and *Nfat1*$^{-/-}$*Nfat2*$^{fl/fl}$ *Cd4cre* T cells w/o Tregs: all >18 d. Statistical significance was calculated using Student's *t* test (*B and C*); *$P < 0.05$, **$P < 0.01$, ***$P < 0.001$.

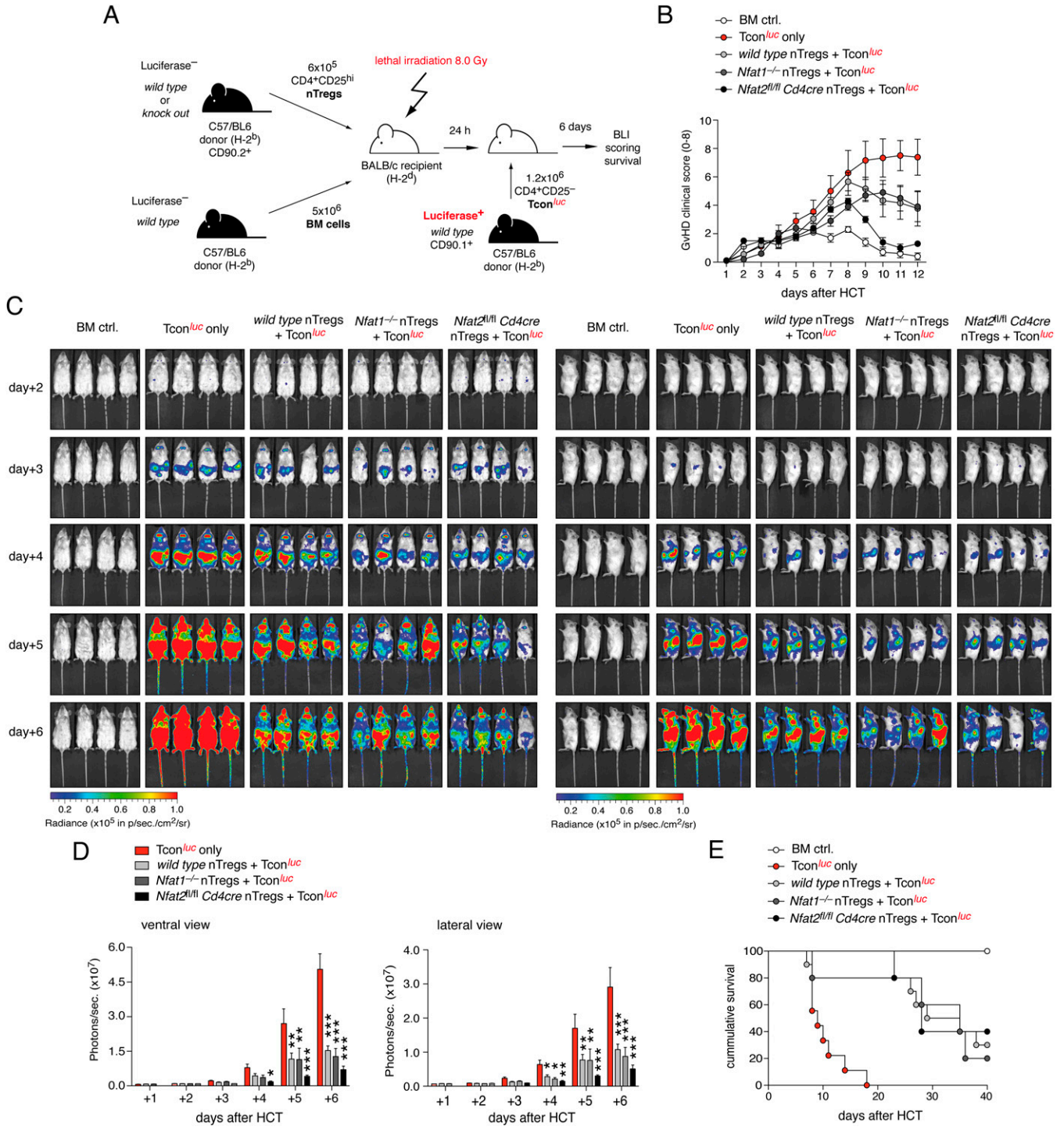

Fig. S6. Adoptive transfer of NFAT-deficient Foxp3$^+$ Tregs limits GvHD pathology. (*A*) Model of nTreg-mediated protection from acute GvHD. BALB/c (H-2^d) mice were lethally irradiated with a single dose of 8.0 Gy and transplanted the same day with 5×10^6 CD90.2$^+$ BM cells and 6×10^5 CD90.1$^+$ luciferase$^-$ CD4$^+$ CD25^{hi} nTregs from WT, *Nfat1*$^{-/-}$, or *Nfat2*$^{fl/fl}$ *Cd4cre* BL/6 donors (H-2^b). 24 h later, mice were infused with 1.2×10^6 CD90.1$^+$luciferase$^+$ WT CD4$^+$CD25$^-$ Tcon cells (H-2^b). (*B*) Clinical scoring for GvHD symptoms (score 0–8) of mice ($n = 5$) transplanted with 1.2×10^6 Tcon plus 5×10^6 BM cells alone (Tcon only) or in combination with 6×10^5 CD4$^+$CD25^{hi} nTregs from luciferase$^-$ WT, *Nfat1*$^{-/-}$, or *Nfat2*$^{fl/fl}$ *Cd4cre* donors. (*C*) Representative in vivo BLI of mice transplanted with 1.2×10^6 luciferase$^+$ WT Tcon plus 5×10^6 BM cells alone or in combination with 6×10^5 CD4$^+$CD25^{hi} nTregs from luciferase$^-$ WT, *Nfat1*$^{-/-}$, or *Nfat2*$^{fl/fl}$ *Cd4cre*, ventral (*Left*) and lateral view (*Right*). (*D*) Quantification of BLI data from two independent experiments with five mice per group per experiment as shown in *C*. (*E*) Cumulative survival of mice transplanted with WT luciferase$^+$ Tcon minus ($n = 10$) or plus CD4$^+$CD25^{hi} nTregs from luciferase$^-$ WT ($n = 10$), *Nfat1*$^{-/-}$ ($n = 5$), or *Nfat2*$^{fl/fl}$ *Cd4cre* ($n = 5$) donors. Median survival: BM ctrl: >40 d; Tcon only: 9 d; Tcon + WT nTregs: 32 d; Tcon + *Nfat1*$^{-/-}$ nTregs: 35 d; Tcon + *Nfat2*$^{fl/fl}$ *Cd4cre* nTregs: 28 d. Statistical significance by two-way ANOVA (*B*); $^*P < 0.05$, $^{**}P < 0.01$, $^{***}P < 0.001$.

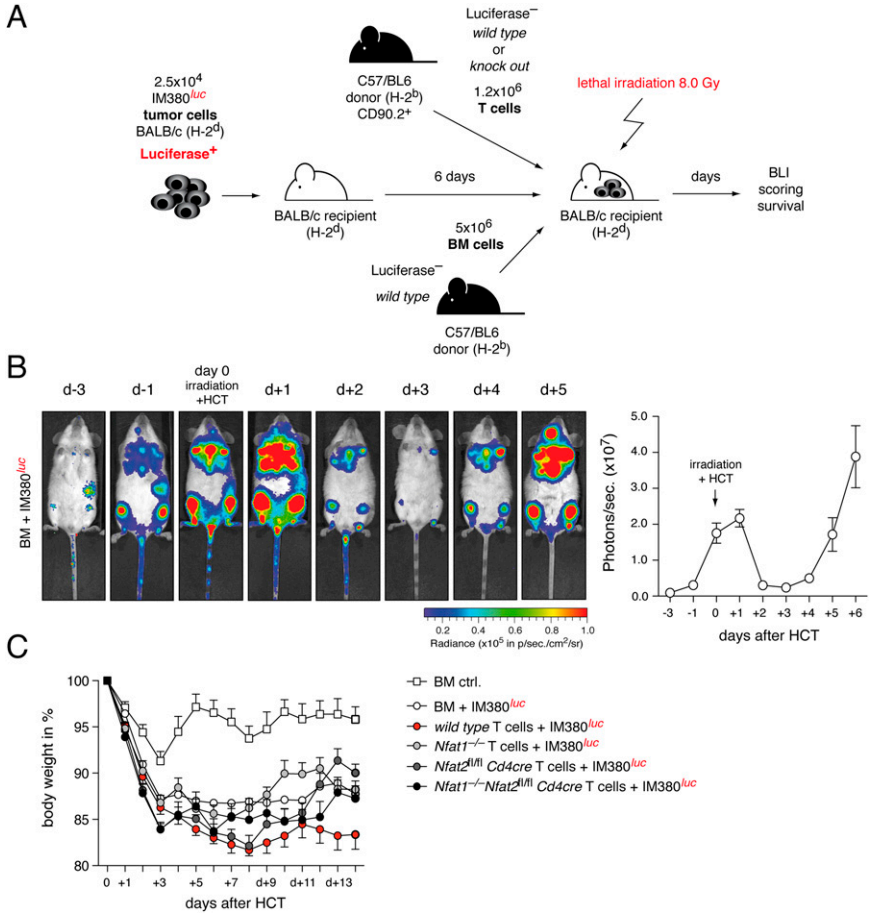

Fig. S7. Intact GvL activity of NFAT-deficient T cells. (*A*) Model of a preestablished tumor for testing GvL activity of transplanted allogenic T cells. Six days before allo-HCT, mice were infused with 2.5×10^4 syngenic IM380 luciferase$^+$ lymphoma cells (H-2^d). Subsequently, mice with established lymphomas were lethally irradiated with a single dose of 8.0 Gy and transplanted with 5×10^6 BM cells and 1.2×10^6 luciferase$^-$ T cells from allogenic C57BL/6 donors (H-2^b). (*B*) Representative BLI pictures of mice transplanted with luciferase$^+$ IM380 tumor cells before and after lethal irradiation and transfer of BM cells (*Left*). Quantification of BLI data ($n = 5$) from days −3 to +6 after allo-HCT, demonstrating initial tumor growth, irradiation-mediated contraction, and relapse of the tumor (*Right*). (*C*) Body weight changes of mice transplanted with 2.5×10^4 IM380 tumor cells alone ($n = 15$) or with 1.2×10^6 allogenic WT ($n = 15$), *Nfat1*$^{-/-}$ ($n = 10$), *Nfat2*$^{fl/fl}$ *Cd4cre* ($n = 10$), or *Nfat1*$^{-/-}$*Nfat2*$^{fl/fl}$ *Cd4cre* T cells ($n = 10$). Mice without IM380 tumor cells but transfer of 5 x10^6 allogenic BM cells ($n = 5$) were used as control.

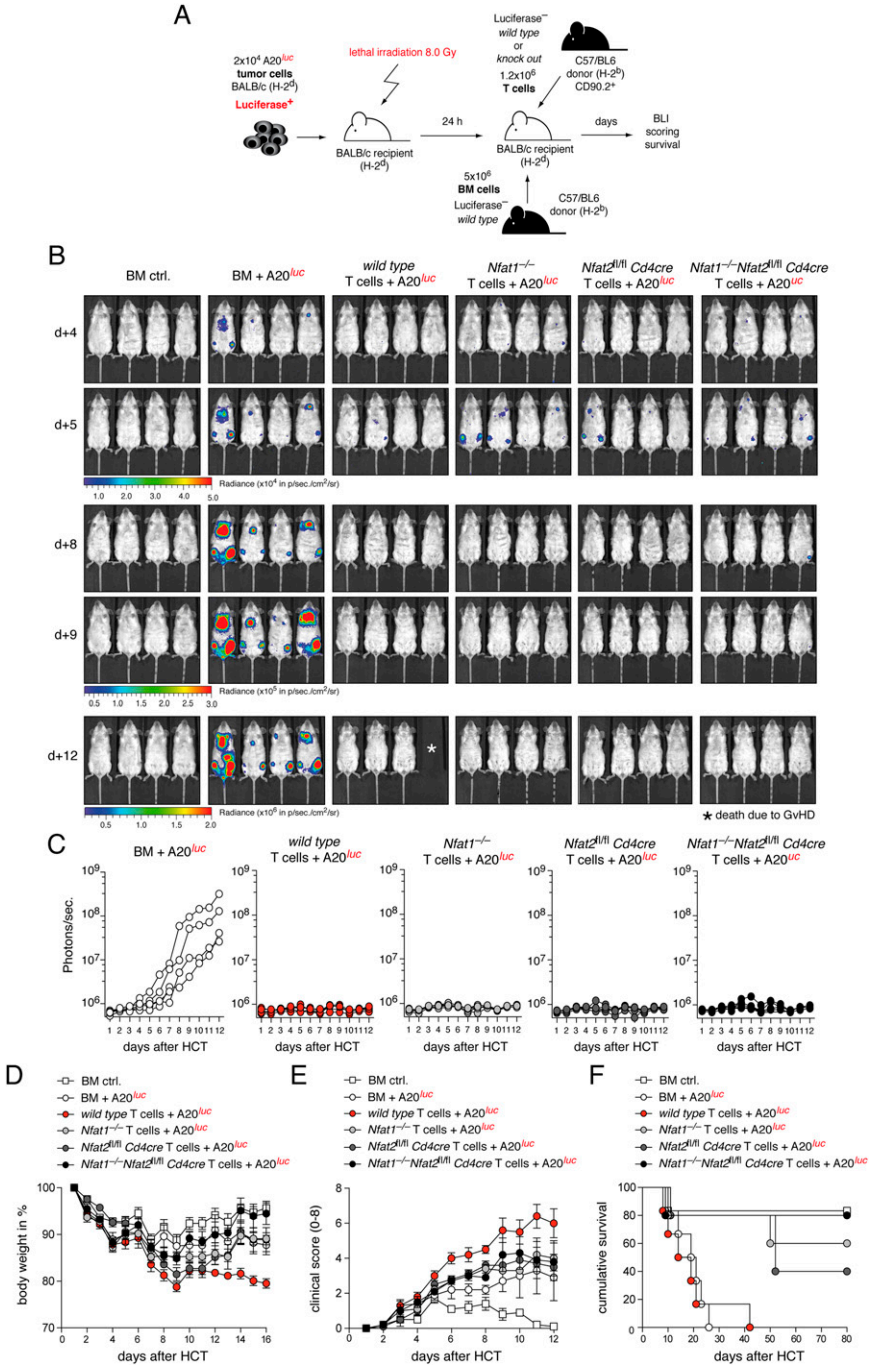

Fig. S8. Intact GvL activity of NFAT-deficient T cells in an A20 B-cell leukemia model. (*A*) A20 B-cell leukemia tumor model for testing GvL activity. The 2×10^4 luciferase$^+$ A20 B-cell leukemia cells (H-2^d) were injected i.v. after TBI with 8.0 Gy. Twenty-four hours later, mice were transplanted with 5×10^6 T-cell–depleted BM cells and 1.2×10^6 luciferase$^-$ T cells from C57BL/6 donors (H-2^b). (*B*) Representative BLI pictures of mice transplanted with luciferase$^+$ A20 tumor cells alone or together with 1.2×10^6 allogenic WT, *Nfat1*$^{-/-}$, *Nfat2*$^{fl/fl}$ *Cd4cre*, or *Nfat1*$^{-/-}$*Nfat2*$^{fl/fl}$ *Cd4cre* T cells. Mice without A20 tumor cells but transfer of 5×10^6 allogenic BM cells were used as control. Asterisk: death due to acute GvHD. (*C*) Quantification of BLI data ($n = 5$) over 12 d after allo-HCT as shown in *B*. (*D* and *E*) Body weight changes (*D*) and clinical scoring (*E*) of mice transplanted with 2×10^4 A20 tumor cells (BM + A20; $n = 10$) without or with 1.2×10^6 allogenic WT ($n = 10$), *Nfat1*$^{-/-}$ ($n = 10$), *Nfat2*$^{fl/fl}$ *Cd4cre* ($n = 10$), or *Nfat1*$^{-/-}$*Nfat2*$^{fl/fl}$ *Cd4cre* T cells ($n = 10$). Mice without A20 tumor but transfer of 5×10^6 allogenic BM cells (BM ctrl; $n = 5$) were used as control. (*F*) Survival of mice inoculated with 2×10^4 A20 luciferase$^+$ tumor cells alone (BM + A20) or transplanted with 1.2×10^6 allogenic WT ($n = 10$), *Nfat1*$^{-/-}$ ($n = 10$), *Nfat2*$^{fl/fl}$ *Cd4cre* ($n = 10$), and *Nfat1*$^{-/-}$*Nfat2*$^{fl/fl}$ *Cd4cre* ($n = 10$) T cells. As a control, mice were transplanted with BM cells only (BM ctrl; $n = 5$). Median survival: BM + A20: 20 d; WT + A20: 16.5 d; *Nfat2*$^{fl/fl}$ *Cd4cre* + A20: 52 d; *Nfat1*$^{-/-}$ + A20, *Nfat1*$^{-/-}$*Nfat2*$^{fl/fl}$ *Cd4cre* + A20, and BM ctrl: >80 d.

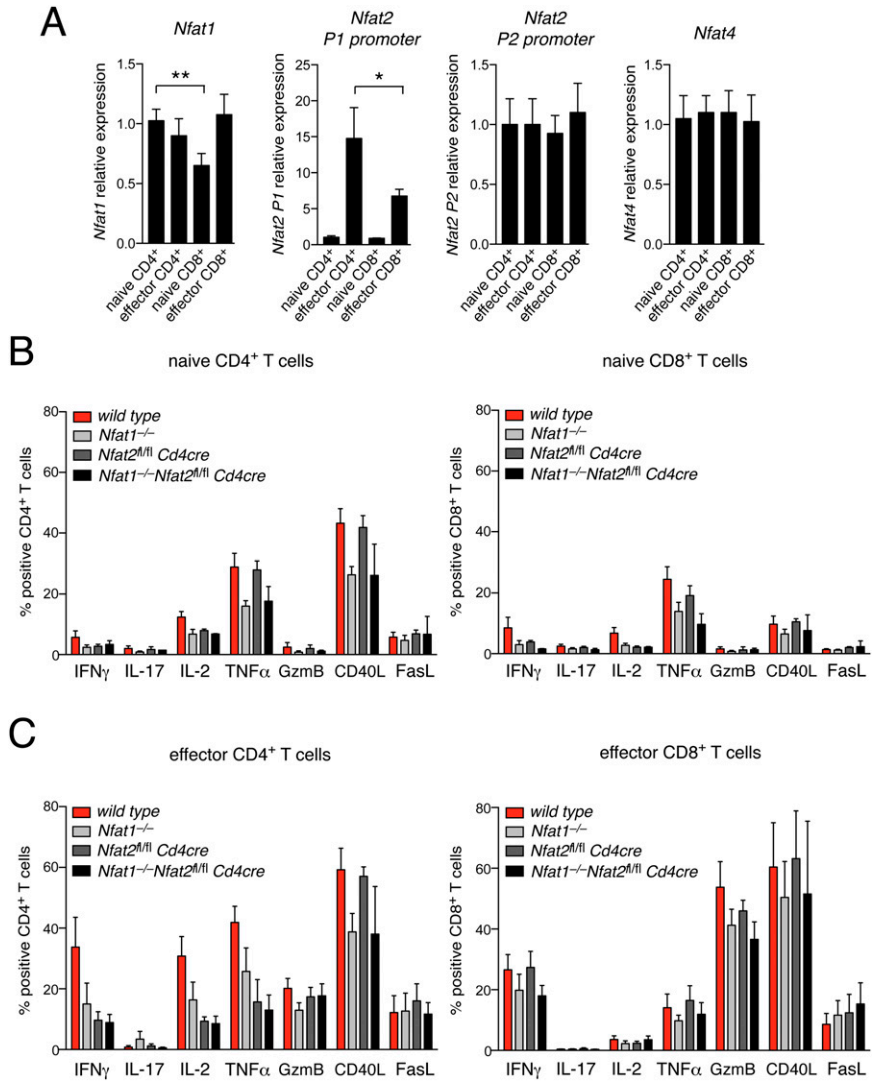

Fig. S9. Expression and function of NFAT1 and NFAT2 in $CD4^+$ and $CD8^+$ T cells. (*A*) Expression of *Nfat1*, *Nfat2* (P1 and P2 promoter-directed transcripts), and *Nfat4* in $CD44^-CD62L^{hi}$ naïve and $CD44^{hi}CD62L^-$ effector $CD4^+$ and $CD8^+$ T cells analyzed by qRT-PCR. (*B*) Expression of IFNγ, IL-17, IL-2, TNFα, GzmB, CD40L, and FasL in freshly isolated $CD4^+$ (*Left*) and $CD8^+$ T cells (*Right*). $CD4^+$ and $CD8^+$ T cells from WT ($n = 5$), *Nfat1*$^{-/-}$ ($n = 4$), *Nfat2*$^{fl/fl}$ *Cd4cre* ($n = 4$), or *Nfat1*$^{-/-}$*Nfat2*$^{fl/fl}$ *Cd4cre* mice ($n = 2$) were stimulated with TPA/iono for 6 h and analyzed by flow cytometry. (*C*) Expression of IFNγ, IL-17, IL-2, TNFα, GzmB, CD40L, and FasL in $CD4^+$ (*Left*) and $CD8^+$ T cells (*Right*) that were expanded in vitro for 3 d under Th1 conditions. $CD4^+$ and $CD8^+$ T cells from WT ($n = 9$), *Nfat1*$^{-/-}$ ($n = 9$), *Nfat2*$^{fl/fl}$ *Cd4cre* ($n = 7$), or *Nfat1*$^{-/-}$*Nfat2*$^{fl/fl}$ *Cd4cre* mice ($n = 6$) were restimulated with TPA/iono for 6 h and cytokines were analyzed by flow cytometry. Statistical significance was calculated using Student's *t* test; $*P < 0.05$, $**P < 0.01$.

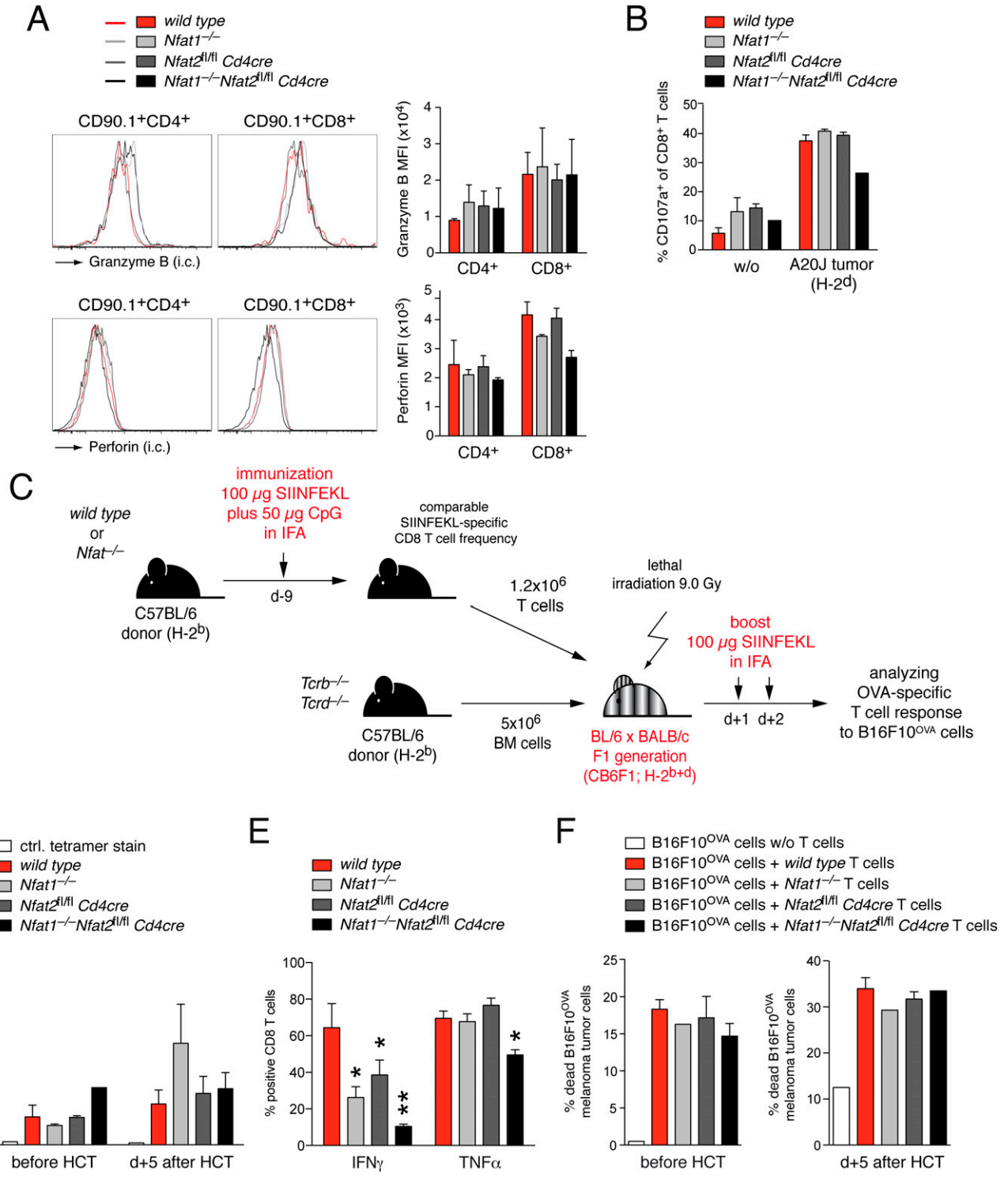

Fig. S10. NFAT-deficient donor T cells confer CD8$^+$ T-cell memory after semiallo-HCT. (*A*) Expression of granzyme B and perforin in donor-derived CD90.1$^+$ CD4$^+$ and CD90.1$^+$CD8$^+$ T cells. BALB/c host mice were transplanted with 1.2×10^6 allogenic WT, *Nfat1*$^{-/-}$, *Nfat2*$^{fl/fl}$ *Cd4cre*, and *Nfat1*$^{-/-}$*Nfat2*$^{fl/fl}$ *Cd4cre* T cells and 5×10^6 BM cells. Six days later, expression of intracellular granzyme B and perforin in donor CD4$^+$ and CD8$^+$ T cells was analyzed by flow cytometry; representative histograms of granzyme B and perforin staining (*Left*) and quantification of five mice per group (*Right*). (*B*) CD8$^+$ T cells from WT, *Nfat1*$^{-/-}$, *Nfat2*$^{fl/fl}$ *Cd4cre*, and *Nfat1*$^{-/-}$*Nfat2*$^{fl/fl}$ *Cd4cre* C57BL/6 (H-2^b) mice were expanded for 3 d under Th1 conditions. Cultured cells were incubated with or w/o allogenic A20 tumor cells (H-2^d) for 2 h and surface expression of CD107a (LAMP-1) was analyzed by flow cytometry. (*C*) Mouse model for testing protective CD8$^+$ T cells memory after semiallogenic transplantation. 9 d before transplantation, WT, *Nfat1*$^{-/-}$, *Nfat2*$^{fl/fl}$ *Cd4cre*, and *Nfat1*$^{-/-}$*Nfat2*$^{fl/fl}$ *Cd4cre* mice were immunized s.c. with 100 μg SIINFEKL OVA-peptide and 50 μg CpG emulsified in IFA. The 1.2×10^6 T cells of SIINFEKL-immunized C57BL/6 (H-2^b) mice were then transplanted into semiallogenic CB6F1 (C57BL/6 × BALB/c F1 hybrid, H-2^{b+d}) host mice together with 5×10^6 *Tcrb*$^{-/-}$*Tcrd*$^{-/-}$ C57BL/6 BM cells. CB6F1 host mice were boosted i.v. with 100 μg SIINFEKL OVA peptide in IFA on days +1 and +2 after semiallo-HCT. Frequency of SIINFEKL-specific CD8$^+$ T cells, cytokine production, and memory response to OVA-expressing C57BL/6 melanoma cells (B16F10^{OVA}) was tested at day +6. (*D*) Detection of SIINFEKL-specific of CD8$^+$ T

Legend continued on following page

cells using a SIINFEKL-loaded H-2^b tetramer by flow cytometry. Analysis was done before HCT and 6 d after semiallo-HCT; as a reference for gating, a control tetramer staining was used. (*E*) Representative intracellular flow cytometry detecting IFNγ and TNFα expression of splenic $CD8^+$ T cells 6 d after semiallo-HCT as described in *C*. Total spleen cells were restimulated for 6 h with TPA/iono; data are summarized from four to eight mice per group. (*F*) Testing OVA-specific $CD8^+$ T-cell memory response 5 d after semiallo-HCT. Splenocytes from CB6F1 host mice transplanted with SIINFEKL-immunized WT, *Nfat1*$^{-/-}$, *Nfat2*$^{fl/fl}$ *Cd4cre*, and *Nfat1*$^{-/-}$*Nfat2*$^{fl/fl}$ *Cd4cre* T cells (C57BL/6, H-2^b) were incubated with OVA-expressing B16F10 melanoma cells (B16F10^{OVA}, H-2^b). Dead B16F10^{OVA} melanoma cells were analyzed 4 h later by propidium iodide staining using flow cytometry. Statistical significance was calculated using Student's *t* test (*A and E*); $*P < 0.05$, $**P < 0.01$.